Electrochemical Investigation of the Corrosion Resistance of Ti20Mo Alloys in Simulated Physiological Solution with Added Proteins for Biomaterial Application

D. Mareci[1], B.M. Fernández-Pérez[2], L.C. Trinca[3,*], L. Fotea[3], R.M. Souto[2,4,*]

[1] Technical University "Gheorghe Asachi" of Iasi, D.Mangeron, Iasi, 700050, Romania.
[2] Department of Chemistry, Universidad de La Laguna, E-38205 La Laguna (Tenerife, Canary Islands), Spain.
[3] "Ion Ionescu de la Brad" University of Agricultural Science and Veterinary Medicine, Faculty of Horticulture, Science Department, 3, Mihail Sadoveanu Alley, Iaşi, 700490, Romania.
[4] Institute of Material Science and Nanotechnology, Universidad de La Laguna, E-38200 La Laguna (Tenerife, Canary Islands), Spain.
[*]E-mail: lctrinca@Yahoo.com, rsouto@ull.es

Corrosion behaviour of the studied Ti20Mo alloy together with the currently used metallic biomaterials Ti6Al4V, and Ti6Al7Nb alloys was investigated for biomedical applications. All the samples were examined using electrochemical techniques: linear polarization curves and electrochemical impedance spectroscopy (EIS) in electrochemical media: Ringer's solution with proteins at 37 °C. The passive behaviour for all the Ti samples is observed for Ringer's solution with proteins. The Ti20Mo alloy underwent spontaneous passivation, and exhibited more positive zero current potential (E_{ZCP}), and lower corrosion current densities (j_{corr}) than Ti6Al4V, and Ti6Al7Nb alloys. The Ti20Mo alloy appears to posses superior corrosion resistance in Ringer's solution with proteins than the Ti6Al4V, and Ti6Al7Nb biomaterials.

1. INTRODUCTION

There is major demand for replacement of failed tissues and organs by biomaterials and artificial devices due to the combination of longer life expectancies and increased sport activities

among the population [1]. For example, an 8% annual growth is anticipated in the orthopedic industry from $6 billion in 2007 to $13 billion by 2017 [2]. To meet this demand, a wide variety of materials comprising polymers, ceramics, and metals are being developed.

Titanium and its alloys are one of the most widely studied and used metallic biomaterials. These materials consistently remain the first choice for implants in both medical and dental applications due to their biological advantages and excellent corrosion resistance [3-5]. Though "commercially pure" grades (II–IV) of Ti (CPTi) are still used particularly in dentistry, most orthopaedic devices are fabricated from Ti6Al4V alloy (ASTM F-1472, ASTM F-136, ISO 5832-3), followed by vanadium-free α+β type alloys such as Ti6Al7Nb (ASTM F-1295, ISO 5832-11). Titanium is non-toxic and fairly unreactive in physiological environments [6,7], but analysis of tissues adjacent to implant materials shows that titanium accumulates in giant cells and is not excreted [8-10]. Conversely, vanadium and aluminium are tolerated by the human organism only to a moderate degree [11]. Furthermore, reports have shown that V, used to stabilize the β-phase, produces harmful oxides for the human body [12,13]. According to Piazza et al. [14], Al is poorly absorbed within the gastrointestinal tract, very little gets into the blood stream, but has been concerned, not yet confirmed, about the association between Al and Alzheimer disease [15,16]. Therefore, in recent years, attempts were made to develop new titanium alloys for medical implants without V and Al [15] with β-Ti alloys being envisaged to become promising candidates for biomedical applications [17-20]. Thus, β-type titanium alloys with biomechanical compatibility, low modulus and biochemical compatibility are envisaged [1,21,22]. The β-stabilizing elements, such as Mo, Ta, and Sn are selected as safe alloying elements to titanium, which are judged to be non-toxic and non-allergic [1].

This contribution reports on the characterization of Ti20Mo alloy with the objective to design new biomedical metastable β-type titanium alloy with improved corrosion resistance. It has been recently shown that Ti20Mo composition showed the highest corrosion resistance in terms of passivation characteristics in simple saline solutions [23-25]. Yet, some reports have shown that the presence of protein may have negative [26] or positive influence [27-30] on the corrosion resistance of Ti and its alloys. Therefore, proteins are of importance in biomaterials biocompatibility and surface degradation, and they have been added to the simulated physiological environment employed to characterize the corrosion resistance of the new Ti20Mo alloy. In order to assist to establish the potential of the new Ti20Mo alloy for biomaterial application, its corrosion resistance was compared with Ti6Al4V and Ti6Al7Nb alloys under the same experimental conditions.

2. MATERIALS AND METHODS

The Ti20Mo alloy was synthesized by cold crucible levitation melting technique in a high frequency induction furnace under a pure Ar atmosphere, which was introduced after several cycles of high vacuum pumping as described elsewhere [31]. Ti6Al4V and Ti6Al7Nb alloys were obtained from a bar stock in annealed state. The supplier and nominal chemical compositions of the three alloys are shown in Table 1.

Table 1. Origin and chemical composition of investigated Ti-based alloys.

Samples	Composition (wt %)	Supplier
Ti6Al4V	Ti: 90, Al: 6, V: 4	IMNR, Romania[*]
Ti6Al7Nb	Ti: 87, Al: 6, Nb: 7	IMNR, Romania[*]
Ti20Mo	Ti: 80, Mo: 20	INSA Rennes, France[**]

[*] National Institute of Research & Development for Non-ferrous and Rare Metals, Bucharest, Romania
[**] INSA Rennes, France

The samples were cut to obtain a 0.95 cm^2 flat surface that was ground with SiC abrasive paper up to 2000 grit, followed by polishing with 1 μm alumina suspension. Subsequently the samples were degreased with ethyl alcohol, followed by ultrasonic cleaning with deionised water and dried under air stream. The microstructures of the alloys were characterized by optical microscopy using a Leica DM RM system (Wetzlar, Germany).

Electrochemical tests were conducted in aerated physiological Ringer's solution whose composition was: NaCl: 8.6 g/L, KCl: 0.3 g/L, CaCl$_2$: 0.48 g/L, with added 37.5 mg/mL human albumin protein (Kedrion S.p.A. Barga, Italy). The pH was measured with a multi-parameter analyser Consort 831C (Turnhout, Belgium). The pH of this medium was 7.3 ± 0.1.

Electrochemical measurements were carried out in aerated solution at 37 ± 1°C using a potentiostat model PARSTAT 4000 (Princeton Applied Research, Princeton, NJ, USA). The instrument was controlled by a personal computer and *Versa Studio* software. A glass corrosion cell kit with a platinum counter-electrode and a saturated calomel reference electrode (SCE) were used to perform the electrochemical measurements. The EIS spectra were recorded in the 10^{-2} Hz to 10^5 Hz frequency range. The applied alternating potential signal had amplitude of 10 m V. In order to supply quantitative support for discussions of these experimental EIS results, an appropriate model (*ZSimpWin*, Princeton Applied Research, Princeton, NJ, USA) for equivalent circuit (EC) quantification was used.
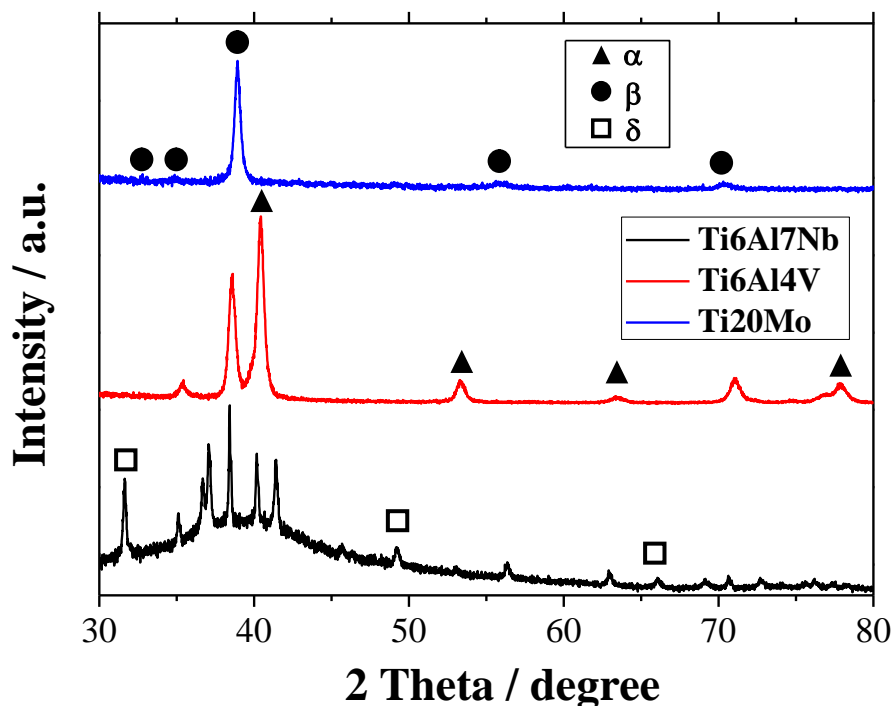
The linear potentiodynamic polarization tests were initiated after 7 days immersion of the samples in aerated Ringer's solution with proteins at 37 ^{o}C. The tests were conducted by scanning the potential, at the rate of 1 mV s^{-1}, from -1.0 V$_{SCE}$ up to +1.0 V$_{SCE}$. Standard techniques were used to extract the zero current potential (E_{ZCP}), and the corrosion current density (j_{corr}), namely the application of Tafel analysis for a range of ±100 mV around the open circuit potential. From the measured potentiodynamic polarization curves, the passive current density (j_{pass}) was determined too.

The surface morphology of the specimens after electrochemical testing was observed by scanning electron microscopy. SEM observations were made using a Quanta 200 (FEI, Hillsboro, OR, USA) operated at an accelerating voltage of 30 kV.
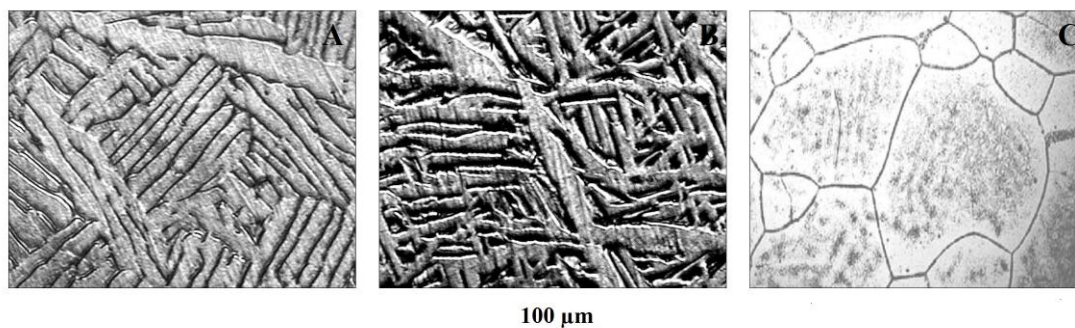
3. RESULTS AND DISCUSSION

3.1. Microstructural characterization

Quantitative phase analysis by X-ray diffraction showed that the dominant phase for the new alloy Ti20Mo is the β solid solution as shown in Figure 1. The X-ray patterns for the Ti6Al4V and Ti6Al7Nb alloys are also given in the figure for comparison.

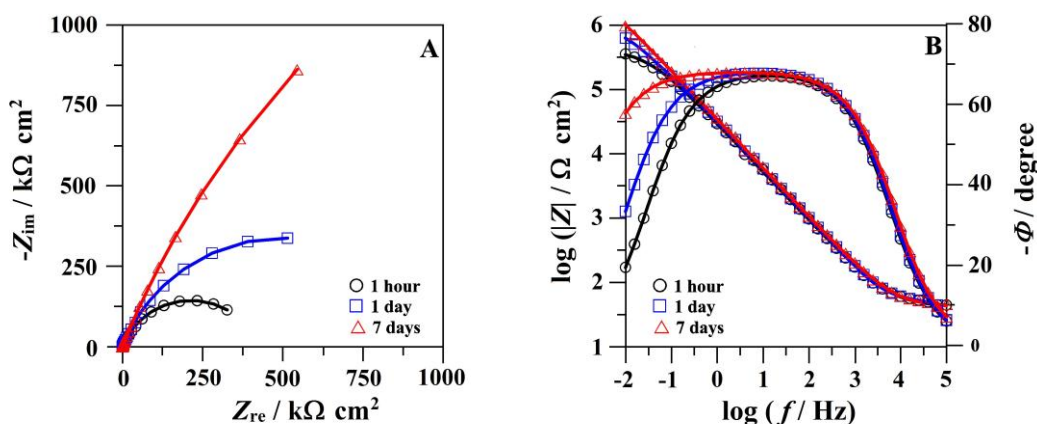**Figure 1.** XRD patterns of Ti6Al4V, Ti6Al7Nb, and Ti20Mo alloys.

Figure 2. Optical micrographs of the alloys: (A) Ti6Al4V, (B) Ti6Al7Nb, and (C) Ti20Mo.

The microstructures of the three materials are shown in Figure 2, showing major morphological differences between the binary Ti20Mo alloy and Ti6Al4V, and Ti6Al7Nb alloys. The optical
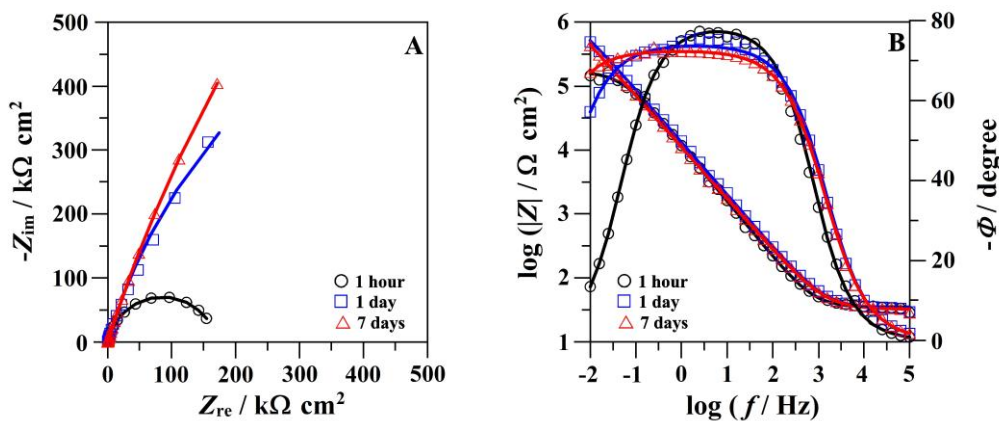
micrographs for the ternary alloys showed that the morphology of the dominant solid solution has a two-phase structure, with coarse β-phase grains containing lamellar α-phase, originating a basketweave appearance (cf. Figure 2A-B). The developed structure is of Widmansttaten type. Conversely, the micrograph depicted in Figure 2C shows the microstructure of the Ti20Mo alloy to be composed of β equiaxial grains, in good agreement with the XRD observations.

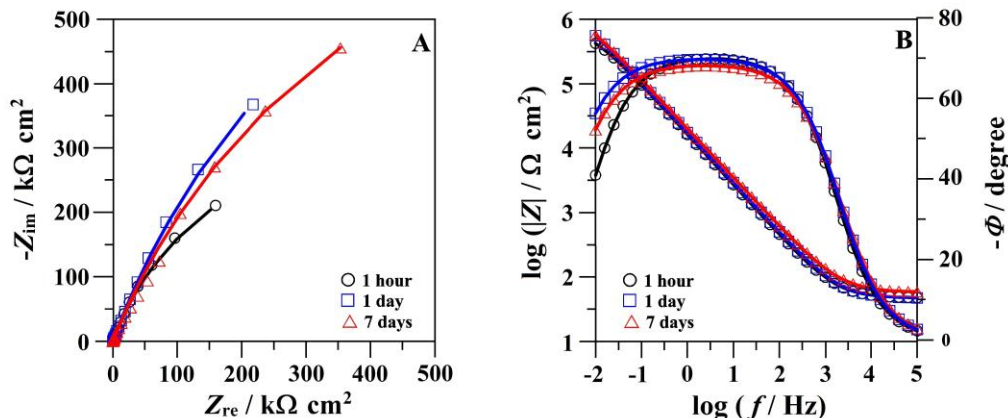### 3.2. Electrochemical impedance spectroscopy

Electrochemical impedance spectroscopy (EIS) is a very useful technique for studying the corrosion behaviour of biomaterials. The EIS data of the alloys measured at three different immersion times in the test solution are presented in Figures 3-5 in the form of Nyquist (complex versus real components of the impedance) and Bode plots (impedance modulus and phase angle versus frequency diagrams).

Figure 3. Measured (discrete points) and fitted (solid lines) impedance spectra obtained during immersion of Ti20Mo alloy in Ringer's solution with added human albumin protein at 37 °C.

Figure 4. Measured (discrete points) and fitted (solid lines) impedance spectra obtained during immersion of Ti6Al4V alloy in Ringer's solution with added human albumin protein at 37 °C.
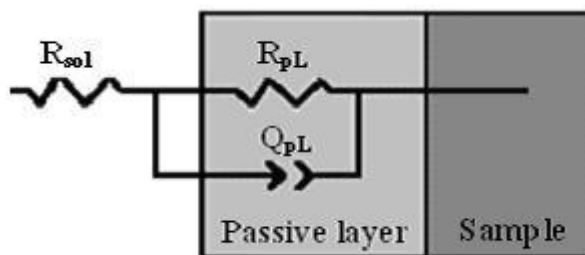
Figure 5. Measured (discrete points) and fitted (solid lines) impedance spectra obtained during immersion of Ti6Al7Nb alloy in Ringer's solution with added human albumin protein at 37 °C.

The maximum phase angles observed for all the samples were found to lie in the range of approximately $-70°$ to $-80°$, a feature indicating the formation of a sealing passivating oxide layer on the alloys at the open circuit potential in Ringer's solution with proteins at 37 °C regardless the length of exposure. High impedance values (order of 10^6 Ω cm^2) were obtained from medium to low frequencies for Ti20Mo alloys at open circuit potential, suggesting high corrosion resistance in this simulated physiological environment.

In all cases, only one time constant is observed in the spectra, and they could be satisfactorily simulated using the simplified Randles' circuit shown in Figure 6, which assumes that the corrosion of the passive Ti-based alloys are hindered by an oxide film that acts as a barrier-type compact layer [32]. This simple EC has been successfully employed to describe the electrochemical behaviour of titanium alloys in various environments under open circuit conditions [33-36], including compact Ti20Mo in saline solution [25], whereas two time constants were required in the case of thicker and aged oxide layers, as they would develop a duplex structure with a porous outer layer [36-40]. This equivalent circuit (EC) contains a series combination of the solution resistance, R_{sol} (around 80 Ω cm^2), with one RQ element in parallel. The parameter R_{pL} coupled with Q_{pL} describes the processes at the inner barrier layer at the electrolyte/compact passive film interface. Since a distributed relaxation feature was observed, a constant phase element (CPE) was used instead of a pure capacitance in the fitting procedure to obtain good agreement between the simulated and experimental data. The impedance of the CPE is given by [41]:

$$Q = Z_{CPE} = \frac{1}{C(j\omega)^n} \tag{1}$$

where, ω is the angular frequency and j is imaginary number ($j^2 = -1$).The parameter n is related to a slope of the log ($|Z|$) vs. log(f) Bode–plots, ω is the angular frequency and j is imaginary number ($j^2 = -1$). Thus, for $n = 1$, the Q element reduces to a capacitor with a capacitance C and, for $n = 0$, to a simple resistor. The quality of fitting to the EC was established first from the χ^2 value that was $< 3 \times 10^{-4}$, and second by the error distribution versus frequency comparing experimental with simulated data. The values of fitted parameters of the EC are presented in Table 2.

Figure 6. Equivalent circuit (EC) used for the interpretation of the measured impedance spectra: one-layer model of a barrier-type compact oxide surface film.

Table 2. EIS fitted results for spectra determined at different exposure durations of the titanium alloys immersed in Ringer's solution with added human albumin protein at 37 °C.

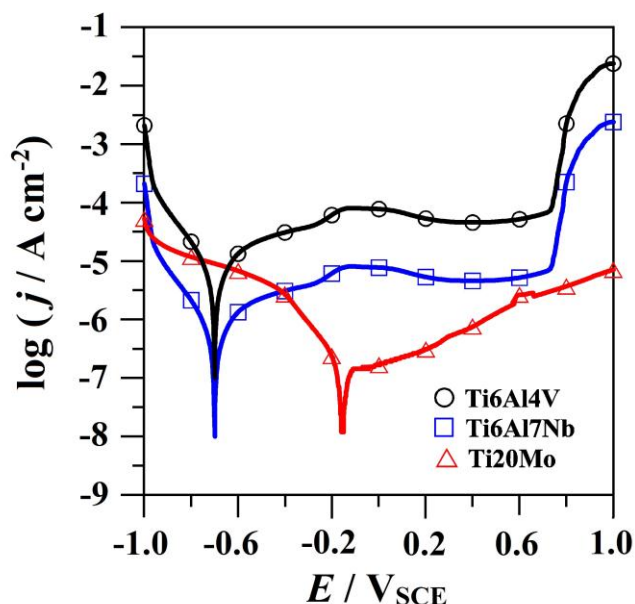| Alloy	Immersion time	Q_{pL} / μS cm^{-2} s^n	n_{pL}	R_{pL} / MΩ cm^2
Ti6Al4V	1 hour	11	0.81	0.2
	1 day	11	0.81	0.3
	7 days	9.9	0.84	0.5
Ti6Al7Nb	1 hour	9.9	0.85	0.4
	1 day	9.8	0.85	0.5
	7 days	9.9	0.86	0.7
Ti20Mo	1 hour	9.8	0.86	0.5
	1 day	9.7	0.86	0.8
	7 days	9.5	0.87	1.2

High values of R_{pL}, in the order of 10^5 -10^6 Ω cm^2, were observed after 7 days of immersion under open circuit potentials for all the Ti-based alloys, confirming the formation of a compact layer with high corrosion protection ability in Ringer's solution with proteins at 37 °C. For highly corrosion resistant materials the polarization resistance (i.e., R_{pL} in this work), may even reach 10^6 Ω cm^2 [42]. Then, the passive oxide film can block the access of electrochemically active species to the Ti-based electrode surface, restricting ion diffusion to the surface, and thus reducing the overall corrosion reaction rate. This feature can also justify the observed increase in R_{pL} with increasing immersion time.

In terms of EIS analysis, the Ti20Mo alloy had a better corrosion resistance than Ti6Al7Nb, and Ti6Al4V alloys immersed in Ringer's solution with proteins. Probably, the addition of Mo to the alloy has a positive contribution to the formation of the compact passive oxide film.

3.3. Potentiodynamic polarization

Figure 7 shows typical linear potentiodynamic polarization curves for pure Ti20Mo, Ti6Al4V, and Ti6Al7Nb alloys plotted in a semi-logarithmic presentation. They were recorded after 7 days immersion in Ringer's solution with proteins solution at 37 °C. Average open circuit potential (E_{ZCP})

and corrosion current density (j_{corr}) values determined from the polarization curves are listed in Table 3 for the various alloys tested. None of the materials exhibited a distinctive active–passive transition in the polarization curves following the Tafel region, but they entered directly into a stable passive regime. This feature indicates that the oxide film spontaneously developed at the surface of the alloys upon immersion in the test electrolyte exhibits passivation characteristics, a feature previously observed for titanium metal [36] and Ti-based alloys such as nitinol [43], and Ti-Nb-Hf [44]. It can also be observed that the anodic polarization curve of the Ti20Mo alloy shifts to the positive (noble) direction.

Figure 7. Representative potentiodynamic polarization curves for the Ti-based alloys immersed in Ringer's solution with added human albumin protein at 37 °C for 7 days. Scanning rate: 1 mV s^{-1}.

The values of the passive current density (j_{pass}) were also determined from the potentiodynamic polarization curves. They were taken from the anodic branch of the potential–current density plots at around the middle of the corresponding passive regions for each material, and they are listed also in Table 3. Very low passive current densities (in order of 10^{-6} A cm^{-2}) were determined, indicating a high resistance of all Ti-based samples in Ringer's solution with proteins.
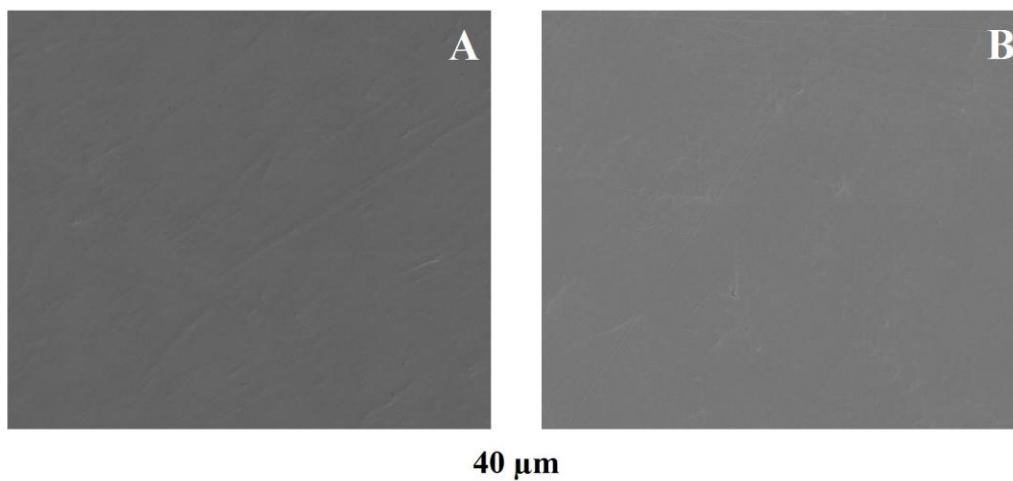
Table 3. Electrochemical parameters from potentiodynamic polarization curves, average of three samples, for the titanium alloys immersed in Ringer's solution with added human albumin protein at 37 °C for 7 days.

Alloy	E_{ZCP} / V$_{SCE}$	j_{corr} / μA cm^{-2}	j_{pass}* / μA cm^{-2}
Ti6Al4V	-0.702 (0.041)	7.1 (0.6)	49 (7)
Ti6Al7Nb	-0.708 (0.035)	0.9 (0.3)	4.5 (0.6)
Ti20Mo	-0.159 (0.016)	0.3 (0.1)	1.6 (0.1)

*Values determined at +0.5 V$_{SCE}$

Figure 8 shows typical SEM images of the resulting surface oxide films after linear polarization in Ringer's solution with proteins for Ti6Al7Nb, and Ti20Mo alloys. That is, they were retrieved after anodic polarization was applied up to +1.0 V_{SCE}. A homogeneous oxide layer was developed at the surface of the titanium alloy samples. Neither pits nor cracks were observed on the surfaces of the alloys after completing the anodic polarization test given in Figure 7. The results reveal a non-predominant corrosion effect of Ringer's solution with proteins on the passive behaviour of these titanium-based alloys.

40 µm

Figure 8. SEM micrographs of: (A) Ti6Al7Nb, and (B) Ti20Mo alloy samples retrieved from Ringer's solution with added human albumin protein for 7 days after recording the potentiodynamic polarization curves depicted in Figure 7.

4. CONCLUSIONS

On the basis of the above results and discussion, the following conclusions are derived:

Passive behaviour is observed for all the Ti-based samples immersed in Ringer's solution with proteins at 37 °C.

Over the frequency range applied for recording the electrochemical impedance spectra, the equivalent circuit (EC) employed for the electrochemical characterization of the Ti alloys that provides the best fitting of the experimental data contains one single time constant. These results evidence the spontaneous formation of a compact oxide layer on the metallic samples that acts as a barrier film and is responsible for the corrosion protection on the surface of the Ti-based samples immersed in Ringer's solution with proteins.

Quantification of the corrosion resistance of these barrier layers in terms of both polarization resistance and passivation current densities support that the addition of Mo for alloying Ti not only promotes the formation of a β-phase microstructure, but it improves the electrochemical corrosion behaviour of Ti-based alloys in Ringer's solution with proteins, as compared to the behaviours of commonly employed biomaterial Ti6Al4V, and Ti6Al7Nb alloys under the same in vitro conditions.

References

1. M. Niinomi, *Sci. Technol. Adv. Mater.*, 4 (2003) 445.
2. P. Gill, N. Munroe, C. Pulletikurthi, S. Pandya and W. Haider, *J. Mater. Eng. Perform.*, 20 (2011) 819.
3. D.F. Williams, in: *Biocompatibility of Clinical Impact Materials*, Vol. 1, D.F. Williams (Ed.); CRC Press, Boca Raton, FL (1981), Ch. 2.
4. P. Kovacs and J.A. Davidson, in: *Medical Applications of Titanium and its Alloys: the Materials and Biological Issues*, S.A. Brown and J.E. Lemons (Eds.); ASTM, West Chonshohocken, PA (1996), p. 163.
5. M. Geetha, A.K. Singh, R. Asokamani and A.K. Gogia, *Prog. Mater. Sci.*, 54 (2009) 397.
6. J. Pan, D. Thierry and C. Leygraf, *Electrochim. Acta*, 41 (1994) 1143.
7. A. Balamurugan, S. Rajeswari, G. Balossier, A.H.S. Rebelo and J.M.F. Ferreira, *Mater. Corros.*, 59 (2008) 855.
8. E. Ingham and J. Fisher, *Proc. Inst. Mech. Eng. H*, 214 (2000) 21.
9. P. Korovessis, G. Petsinis, M. Repanti and T. Repantis, *J. Bone Joint Surg. Am.*, 88 (2006) 1183.
10. J.R. Revell, *J. R. Soc. Interface*, 6 (2008) 1263.
11. S.R. Sousa and M.A. Barbosa, *Clin. Mater.*, 14 (1993) 287.
12. M.A. Khan, R.L. Williams and D.F. Williams, *Biomaterials*, 17 (1996) 2117.
13. T.I. Kim, J.H. Han, I.S. Lee, K.H. Lee, M.C. Shin and B.B. Choi, *Bio-Med. Mater. Eng.*, 17 (1997) 253.
14. S. Piazza, G.L. Biundo, M.C. Romano, C. Sunseri and F. Di Quarto, *Corros. Sci.*, 40 (1998) 1087.
15. Y. Okazaki, Y. Ito, K. Kyo and T. Tateishi, *Mater. Sci. Eng. A*, 213 (1996) 138.
16. S. Rao, Y. Okazaki, T. Tateishi, T. Ushida and Y. Ito, *Mater. Sci. Eng. C*, 4 (1997) 311.
17. H.S. Kim, S.H. Lim, I.D. Yeo and W.Y. Kim, *Mater. Sci. Eng. A*, 449 (2007) 322.
18. Y.L. Zhou, M. Niinomi and T. Akahori, *Mater. Sci. Eng. A*, 483 (2008) 153.
19. Y.L. Zhou and M. Niinomi, *J. Alloys Compd.*, 466 (2008) 535.
20. Y.L. Zhou and M. Niinomi, *Mater. Sci. Eng. C*, 29 (2009) 1061.
21. W.F. Ho, C.P. Ju and J.H. Chern Lin, *Biomaterials*, 20 (1999) 2115.
22. G. He, J. Eckert, Q.L. Dai, M.L. Sui, W. Löser, M. Hagiwara and E. Ma, *Biomaterials*, 24 (2003) 5115.
23. D. Mareci, R. Chelariu, D. M. Gordin, M. Romas, D. Sutiman and T. Gloriant, *Mater. Corros.*, 61 (2010) 829.
24. G. Bolat, D. Mareci, R. Chelariu, J. Izquierdo, S. González and R.M. Souto, *Electrochim. Acta*, 113 (2013) 470.
25. G. Bolat, J. Izquierdo, T. Gloriant, R. Chelariu, D. Mareci and R.M. Souto, *Corros. Sci.*, 98 (2015) 170.
26. M.A. Khan, R.L. Williams and D.F. Williams, *Biomaterials*, 20 (1999) 765.
27. K. Ide, M. Hattori, M. Yoshinari, E. Kawada and Y. Oda, *Dent. Mater.J.*, 22 (2003) 359.
28. H.H. Huang and T. H. Lee, *Dent. Mater.*, 21 (2005) 749.
29. D. Mareci, R. Chelariu, G. Ciurescu, D. Sutiman and T. Gloriant, *Mater. Corros.*, 61 (2010) 768.

30. R. Chelariu, D. Mareci, C. Munteanu, G. Bolat, C. Crimu and I. Zetu, *Dig. J. Nanomater. Bios*, 9 (2014) 1349.
31. D.M. Gordin, E. Delvat, R. Chelariu, G. Ungureanu, M. Besse, M. Laille and T. Gloriant, *Adv. Eng. Mater.*, 10 (2008). 714.
32. J.E.G. Gonzalez and J.C. Mirza-Rosca, *J. Electroanal. Chem.*, 471 (1999) 109.
33. B.L. Wang, Y.F. Zheng and L.C. Zhao, *Mater. Corros.*, 60 (2009) 330.
34. V.A. Alves, R.Q. Reis, I.C.B. Santos, D.G. Souza, T. de F. Gonçalves, M.A. Pereira-da-Silva, A. Rossi and L.A. da Silva, *Corros. Sci.,* 51 (2009) 2473.
35. L.T. Duarte,S.R. Biaggio, R.C. Rocha-Filho and N. Bocchi, *Corros. Sci.,* 72 (2013) 35.
36. R. Chelariu, G. Bolat, J. Izquierdo, D. Mareci, D.M. Gordin, T. Gloriant and R.M. Souto, *Electrochim. Acta,* 137 (2014) 280.
37. E. Alkhateeb and S. Virtanen, *J. Biomed. Mater. Res. A,* 75 (2005) 934.
38. C. Vasilescu, S.I. Drob, E.I. Neacsu and J.C. Mirza Rosca, *Corros. Sci.,* 65 (2012) 431.
39. I. Cvijović-Alagić, Z. Cvijović, J. Bajat and M. Rakin, *Corros. Sci.,* 83 (2013) 245.
40. J. Izquierdo, G. Bolat, D. Mareci, C. Munteanu, S. González and R.M. Souto, *Appl. Surf. Sci.,* 313 (2014) 259.
41. I.D. Raistrick, J.R. Macdonald and D.R. Franceschetti, in: *Theory in Impedance Spectroscopy: Emphasizing Solid Materials and Systems,* J.R MacDonald (Ed.); John Wiley and Sons, New York (1987), p.90.
42. F. Mansfeld, *J. Electrochem. Soc.*, 120 (1973) 515.
43. D. Mareci, R. Chelariu, G. Bolat, A. Cailean, V. Grancea and D. Sutiman, *Trans. Nonferrous Met. Soc.*, 23 (2013) 3829.
44. D. Mareci, R. Chelariu, A. Cailean, F. Brinza, G. Bolat and D.M. Gordin, *Trans. Nonferrous Met. Soc.*, 25 (2015) 345.